Journal of Alloys and Compounds 509 (2011) 8246–8250

Contents lists available at ScienceDirect

Journal of Alloys and Compounds

journal homepage: www.elsevier.com/locate/jallcom

Mn-substituted nickel hydroxide prepared by ball milling and its electrochemical properties

Xiaofeng Li*, Tongchi Xia, Zheng Li, Huichao Dong, Shunyang Li

Henan Provincial Key Laboratory of Surface & Interface, Zhengzhou University of Light Industry, Zhengzhou, 450002 China

ARTICLE INFO

Article history:
Received 21 April 2011
Received in revised form 20 May 2011
Accepted 24 May 2011
Available online 6 June 2011

Keywords:
Nickel hydroxide
Mn substitution
Ball milling
Electrochemical property

ABSTRACT

In order to reduce the price of nickel hydroxide and extend the application of nickel based alkaline secondary batteries, Mn substituted nickel hydroxide ($Ni_{1-x}Mn_x(OH)_2$, x = 0–0.4) was prepared by using a simple ball milling method in this paper. The optimal ball milling conditions were obtained for the preparation of $Ni_{0.8}Mn_{0.2}(OH)_2$. The results of X-ray diffraction, electrochemical impedance spectroscopy and charge–discharge tests indicated that (i) a structure of β-$Ni(OH)_2$ was maintained for $Ni_{1-x}Mn_x(OH)_2$; (ii) the surface electrochemical activity of nickel hydroxide could be effectively improved by Mn substitution; (iii) capacity of $Ni_{0.8}Mn_{0.2}(OH)_2$ reached 282 mA h/g and it showed an excellent cycling durability; (iv) compared to no-substituted nickel hydroxide, $Ni_{0.8}Mn_{0.2}(OH)_2$ showed a decrease both in charge–discharge plateau and capacity; but with the increase of discharge rate, the difference in discharge plateau between them was smaller, and capacity of the latter exceeded the former.

1. Introduction

Nickel hydroxide has been used as positive material in nickel-base alkaline secondary batteries for more than 100 years. Although nickel-base batteries currently meet a strong competition by Li-ion batteries which have higher specific energy, they still occupy a unique position within the battery industry [1–3]. In order to extend the application of these batteries, it is important to reduce the price of nickel hydroxide at the same time improving its performance.

Constituent substitution is an effective way to improve the performance of nickel hydroxide. Mostly used metallic ions are Al^{3+}, Co^{3+}, Fe^{3+} and Mn^{3+}. After being substituted by these trivalent ions, α-$Ni(OH)_2$ with a better reversibility is obtained and can be stable in a strong alkaline solution when the substitution amount (x) exceeds 0.2 [4–7]. Compared to no-substituted $Ni(OH)_2$, the price of these kinds of α-$Ni(OH)_2$ can be obviously lowered except Co-substituted one.

Spherical nickel hydroxide is widely used in alkaline secondary batteries now. It is commonly prepared by a chemical precipitation process with aqueous ammonia as a complexing agent. In order to obtain spherical nickel hydroxide with excellent electrochemical performance, it is crucial to strictly control the pH of the solution during the precipitation course. On the same time, the total preparation time is over 20 h and large amounts of water are consumed.

Recently, a ball milling process has been introduced into the preparation of battery materials, which is a powder processing technique that allows the production of homogeneous materials starting from blended powder mixtures. Some work has been carried out to improve the performance of spherical nickel hydroxide by ball milling [8–10]. The results show that after long time ball milling, nanocrystalline nickel hydroxide powder can be obtained and exhibits superior charge–discharge performance in comparison with untreated spherical $Ni(OH)_2$.

In this paper, in order to reduce the price of nickel hydroxide, Mn-substituted nickel hydroxide ($Ni_{1-x}Mn_x(OH)_2$) was directly prepared by ball milling. Compared to the chemical precipitation method, the ball milling process can be finished in several hours and large amounts of water are saved. On the other hand, different to the above mentioned α-type nickel hydroxide, β-type one was obtained here and its electrochemical properties were discussed in details.

2. Experimental

Ball milling was performed using a planetary ball mill with a 50 ml-capacity stainless steel pot and 50 g stainless steel balls. The ball milling process was separated into two parts. Firstly, a mixture of $NiSO_4 \cdot 6H_2O$ and $MnSO_4 \cdot H_2O$ was added into the pot. The revolution speed was 350–550 rpm min^{-1} and the milling time (mixing time) was 15 min, so as to keep $MnSO_4$ uniformly dispersing in $NiSO_4$. Then NaOH was added into the above spot. Ball milling was operated again with the same revolution speed. The milling time (reaction time) was 15–60 min for the following reaction:

$$(1-x)NiSO_4 + xMnSO_4 + 2NaOH \rightarrow Ni_{1-x}Mn_x(OH)_2 + Na_2SO_4 \quad (1)$$

* Corresponding author. Tel.: +86 371 63556510; fax: +86 371 63556510.
E-mail address: lixiaofeng@zzuli.edu.cn (X. Li).

0925-8388/$ – see front matter © 2011 Elsevier B.V. All rights reserved.
doi:10.1016/j.jallcom.2011.05.096

Table 1
Weights of reaction materials during ball milling process.

Mass ratio of balls to reaction materials	$NiSO_4 \cdot 6H_2O$/g	$MnSO_4 \cdot H_2O$/g	NaOH/g
4:1	8.01	1.29 (x = 0.2)	3.20
	4.74	0 (x = 0)	1.51
	4.38	0.31 (x = 0.1)	1.56
8:1	4.01	0.64 (x = 0.2)	1.60
	3.61	0.99 (x = 0.3)	1.65
	3.18	1.37 (x = 0.4)	1.70
12:1	2.67	0.43 (x = 0.2)	1.07

where x (=0–0.4) was the substitution atomic portion of Mn for nickel in nickel hydroxide. The adding weights of $NiSO_4 \cdot 6H_2O$, $MnSO_4 \cdot H_2O$ and NaOH were shown in Table 1.

The obtained powder was transferred into distilled water and aged at 70 °C for 4 h, and then was washed repeatedly with distilled water until there was no $BaSO_4$ precipitation in the filtrate with the addition of a $BaCl_2$ solution, finally dried at 80–120 °C for use. The powder X-ray diffraction (XRD) was used to analyze the phase structure of the ball milled nickel hydroxide.

The electrochemical properties of the ball milled nickel hydroxide electrodes were investigated in a sandwich-like simulated nickel metal-hydride (Ni-MH) battery containing a 7 mol l^{-1} KOH solution at 25 °C. A hydrogen absorbing alloy (a commercial $MmNi_{3.55}Co_{0.75}Al_{0.2}Mn_{0.5}$ alloy, where Mm is misch metal) electrode with a large capacity was used as the counter electrode. The pasted positive $Ni(OH)_2$ electrodes were made by filling a nickel foam substrate with a mixture of 2 wt.% polytetrafluoroethylene (PTFE) binder, 5 wt.% CoO and 93 wt.% ball milled $Ni(OH)_2$. The pasted electrodes were then dried at 65 °C and pressed to a thickness of 0.65 mm.

The simulated batteries were charged initially at a 0.1 C rate for 15 h and discharged at a 0.2 C rate to a cut-off voltage 1.0 V. Here C corresponds to the current needed to discharge the total capacity of the $Ni(OH)_2$ electrodes in 1 h. Afterward, a cycling test was performed on the batteries by charging at a 0.2 C rate for 7 h and discharging at the same rate to a cut-off voltage 1.0 V for stabilizing their capacity. The batteries were then charged at a 0.2 C rate for 7 h and discharged separately at a 1 C (or 3 C) rate to a cut-off voltage 1.0 V (or 0.9 V) for high-power performance tests. Electrochemical impedance spectroscopy (EIS) tests were performed on the $Ni(OH)_2$ electrodes by using a Solartron Electrochemical Interface model SI1287. Cycle life tests of the $Ni(OH)_2$ electrodes were performed as follows: the simulated batteries were charged at a 1 C rate for 1.2 h, rested for 10 min, then discharged at the same rate to a cut-off voltage 1.0 V.

3. Results and discussion

Nickel hydroxide with different Mn substitution amounts (x = 0–0.4) were prepared at revolution speed 450 rpm min^{-1}, mass ratio of balls to reaction materials 8:1, milling time for reaction 15 min and drying temperature 80 °C. Fig. 1 shows XRD patterns of ball milled nickel hydroxide. Compared to nickel hydroxide without Mn substitution, a structure of β-$Ni(OH)_2$ is maintained for all

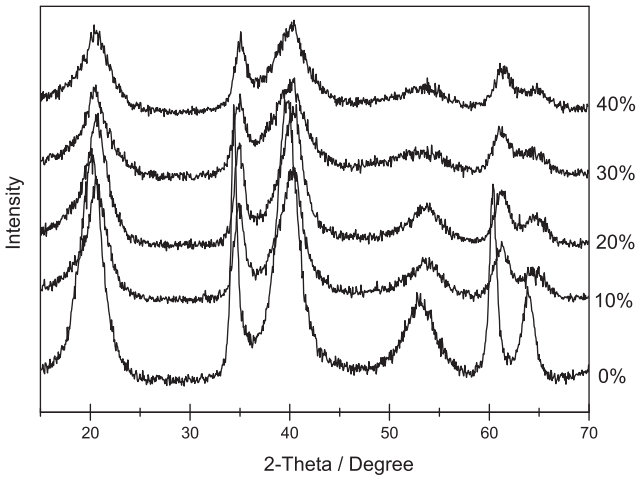

Fig. 1. XRD patterns of ball milled nickel hydroxide with different Mn substituted amount.

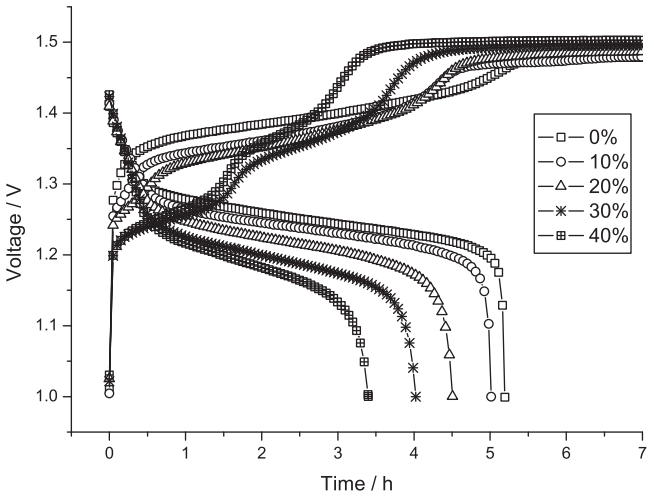

Fig. 2. Typical charge–discharge curves of the simulated Ni-MH batteries at a 0.2 C rate with different Mn substituted amount.

Mn-substituted nickel hydroxide, which is different to α-type Mn-substituted nickel hydroxide prepared by chemical precipitation [5–7]. The diffraction peaks near 20.1°, 34.4° and 39.9° correspond to {0 0 1}, {1 0 0} and {1 0 1} crystal planes, respectively. But the diffraction peaks shift right and their intensity decreases markedly with the increase of substitution amount, which indicates increasing stacking faults and interstratifications in the crystal lattice of nickel hydroxide with the substitution of Mn for nickel [11,12].

Fig. 2 shows the charge–discharge curves of the simulated Ni-MH batteries with ball milled $Ni_{1-x}Mn_x(OH)_2$ (x = 0–0.4) electrodes. Compared to nickel hydroxide without Mn substitution, both discharge plateau and capacity of the batteries with Mn substitution decreases gradually with the increase of the substitution amount. The charge voltage in the early charging stage also shows an obvious decrease for Mn substituted batteries. When the substitution amount (x) exceeds 0.3, a charge plateau appears near 1.2 V, which may be related to the oxidation of Mn ions. These results indicate that the introduction of Mn into the crystal lattice of nickel hydroxide causes a polarization decrease during charge–discharge of the batteries.

Being considered price and the electrochemical properties of nickel hydroxide, the substitution amount x = 0.2 is chosen for further research and ball milling process conditions were discussed in details. Firstly, $Ni_{0.8}Mn_{0.2}(OH)_2$ was prepared at different revolution speeds with mass ratio of balls to reaction materials 8:1, milling time for reaction 15 min and drying temperature 80 °C. Fig. 3 shows the discharge curves of these simulated batteries. The solid phase reaction (1) could not be completely operated both at the lower and higher revolution speeds, since there is not enough energy for the reaction at lower revolution speed and the reaction materials could adhere on the surface of the steel balls at higher one. Thus, 400 rpm min^{-1} is the best revolution speed and the simulated battery shows the largest capacity.

Secondly, the effect of mass ratio of balls to reaction materials was studied. $Ni_{0.8}Mn_{0.2}(OH)_2$ was prepared at different mass ratios with revolution speed 400 rpm min^{-1}, milling time for reaction 15 min and drying temperature 80 °C. Fig. 4 shows the discharge curves of these simulated batteries. Similar to the effects of revolution speed, there is no enough energy for the reaction at lower mass ratio and the reaction materials could adhere on the surface of the steel balls at higher one, therefore, 8:1 is the best mass ratio and the simulated battery shows the largest capacity.

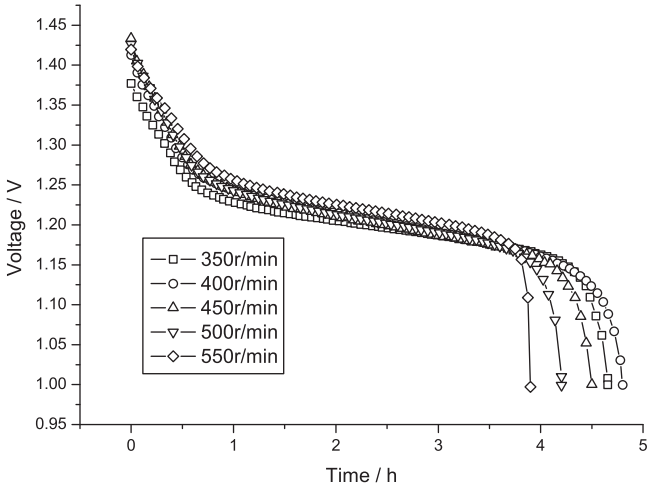

Fig. 3. Typical discharge curves of the simulated Ni-MH batteries at a 0.2 C rate with $Ni_{0.8}Mn_{0.2}(OH)_2$ prepared at different revolution speeds.

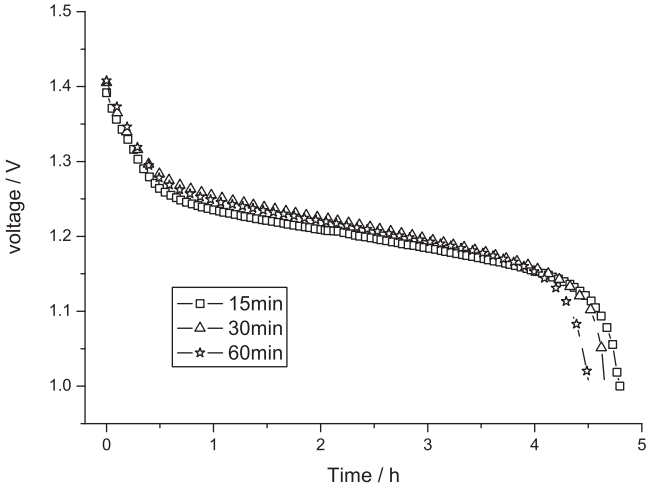

Fig. 6. Typical discharge curves of the simulated Ni-MH batteries at a 0.2 C rate with $Ni_{0.8}Mn_{0.2}(OH)_2$ prepared by different ball milling time for reaction.

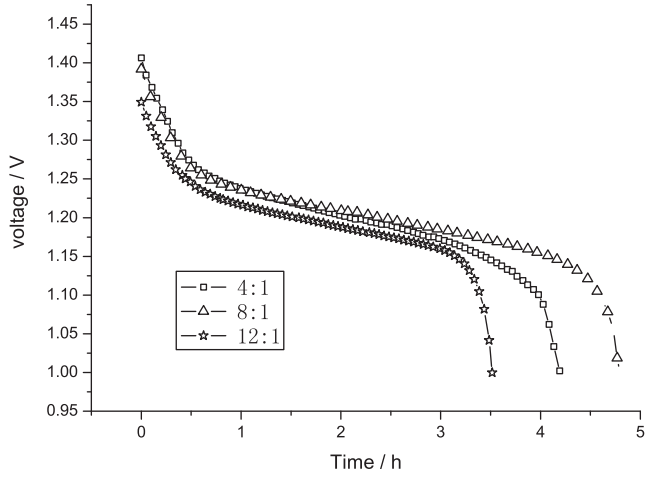

Fig. 4. Typical discharge curves of the simulated Ni-MH batteries at a 0.2 C rate with $Ni_{0.8}Mn_{0.2}(OH)_2$ prepared at different mass ratios of balls to reaction materials.

Next, different milling time for reaction was investigated. Fig. 5 shows XRD patterns of ball milled nickel hydroxide prepared by different milling time for reaction with revolution speed 400 rpm min^{-1}, mass ratio 8:1 and drying temperature 80 °C. As shown in Fig. 5, for $Ni_{0.8}Mn_{0.2}(OH)_2$ prepared by milling time 15 min, the intensity of the diffraction peaks is the strongest and the half peak breadth of {0 0 1}, {1 0 0} and {1 0 1} crystal planes is the narrowest, which indicates it has the better crystallinity. Fig. 6 shows the discharge curves of these simulated batteries. Obviously, 15 min is the best milling time and the simulated battery shows the largest capacity, which is consistent with its best crystallinity.

Finally, the effects of drying temperature on the properties of ball milled $Ni_{0.8}Mn_{0.2}(OH)_2$ were studied. Compared to revolution speed, mass ratio and milling time, the effects of drying temperature are not so notable and the difference among capacity of the batteries is small. The results of Fig. 7 show that 100 °C is the best drying temperature. As the crystal water in nickel hydroxide may play an important role to improve its capacity performance [13], too high drying temperature (>100 °C) results in a capacity decrease.

Thus, the optimal ball milling conditions for $Ni_{0.8}Mn_{0.2}(OH)_2$ are obtained as follows: revolution speed 400 rpm min^{-1}, mass ratio of balls to reaction materials 8:1, milling time for reaction 15 min and drying temperature 100 °C. Then, the electrochemical properties of $Ni_{0.8}Mn_{0.2}(OH)_2$ prepared under the optimal conditions are compared with no-substituted nickel hydroxide. Fig. 8 shows impedance plots of the $Ni(OH)_2$ electrodes discharged to 100% depth of discharge (DOD) in the KOH electrolyte. Clearly, the

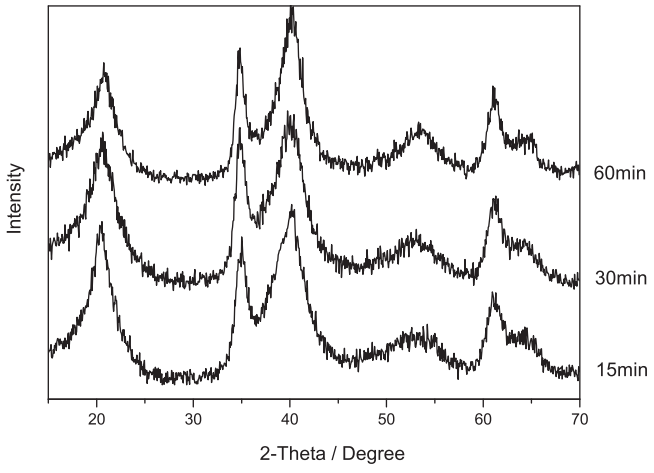

Fig. 5. XRD patterns of ball milled $Ni_{0.8}Mn_{0.2}(OH)_2$ prepared by different ball milling time for reaction.

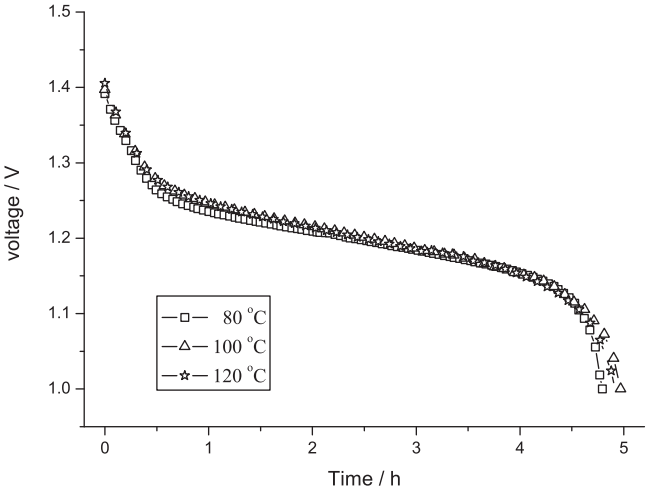

Fig. 7. Typical discharge curves of the simulated Ni-MH batteries at a 0.2 C rate with $Ni_{0.8}Mn_{0.2}(OH)_2$ prepared at different drying temperature.

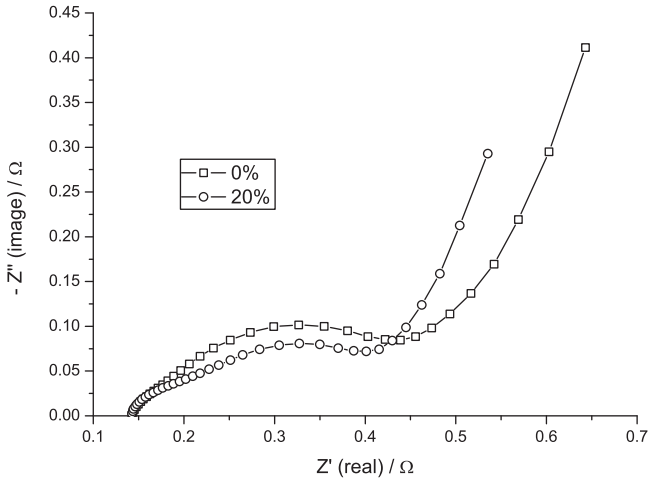

Fig. 8. Impedance plots of $Ni(OH)_2$ electrodes (area = 1 cm^2, loading = 150 mg cm^{-2}, discharged to 100% depth of discharge) in 7 mol l^{-1} KOH electrolyte at a frequency range from 10^5 to 10^{-2} Hz: (a) no-substitution and (b) $Ni_{0.8}Mn_{0.2}(OH)_2$.

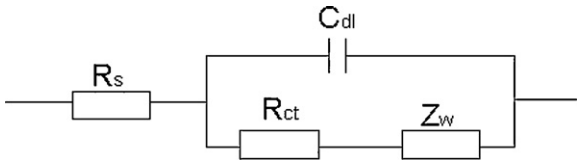

Fig. 9. Proposed equivalent circuit for $Ni(OH)_2$ electrode.

plots exhibit two arcs in the whole frequency range. It is known that the semicircle at high frequency regions corresponds to the charge transfer resistance (R_{ct}) in parallel connection with the double layer capacitance (C_{dl}) and the line at low frequency regions corresponds to the Warburg impedance (Z_w) of proton diffusion [14]. A proposed equivalent circuit for the frequency response of the $Ni(OH)_2$ electrode is given in Fig. 9, where R_s corresponds to the solution resistance. The results of a curve fitting according to the equivalent circuit show a decrease in R_{ct} and increase in C_{dl} (Table 2). Thus, compared to no-substituted nickel hydroxide, the surface electrochemical activity of Mn-substituted one is effective improved.

Fig. 10 shows the discharge curves of the simulated batteries at different discharge rates. The results indicate that with the increase of discharge rate, the difference in discharge plateau between the Mn-substituted battery and no-substituted one becomes smaller, and capacity of the former exceeds the latter at higher discharge rates (>1 C). As Mn-substituted nickel hydroxide shows a better surface electrochemical activity according to the results of Fig. 8, the high-power performance of the simulated battery is improved. The capacity of the $Ni(OH)_2$ electrodes during 300 cycles at a 1 C rate is showed in Fig. 11. Compared to the no-substituted electrode, the Mn-substituted one shows a similar cycling durability. Their capacity after 300 cycles decreases by 4.3% for the latter and 2.8% for the former.

Table 2
Impedance parameters of pasted $Ni(OH)_2$ electrodes in 7 mol l^{-1} KOH electrolyte.

Electrode type	R_{ct}/Ω	C_{dl}/F
No-substituted $Ni(OH)_2$ electrode	0.265	0.596
$Ni_{0.8}Mn_{0.2}(OH)_2$ electrode	0.218	0.729

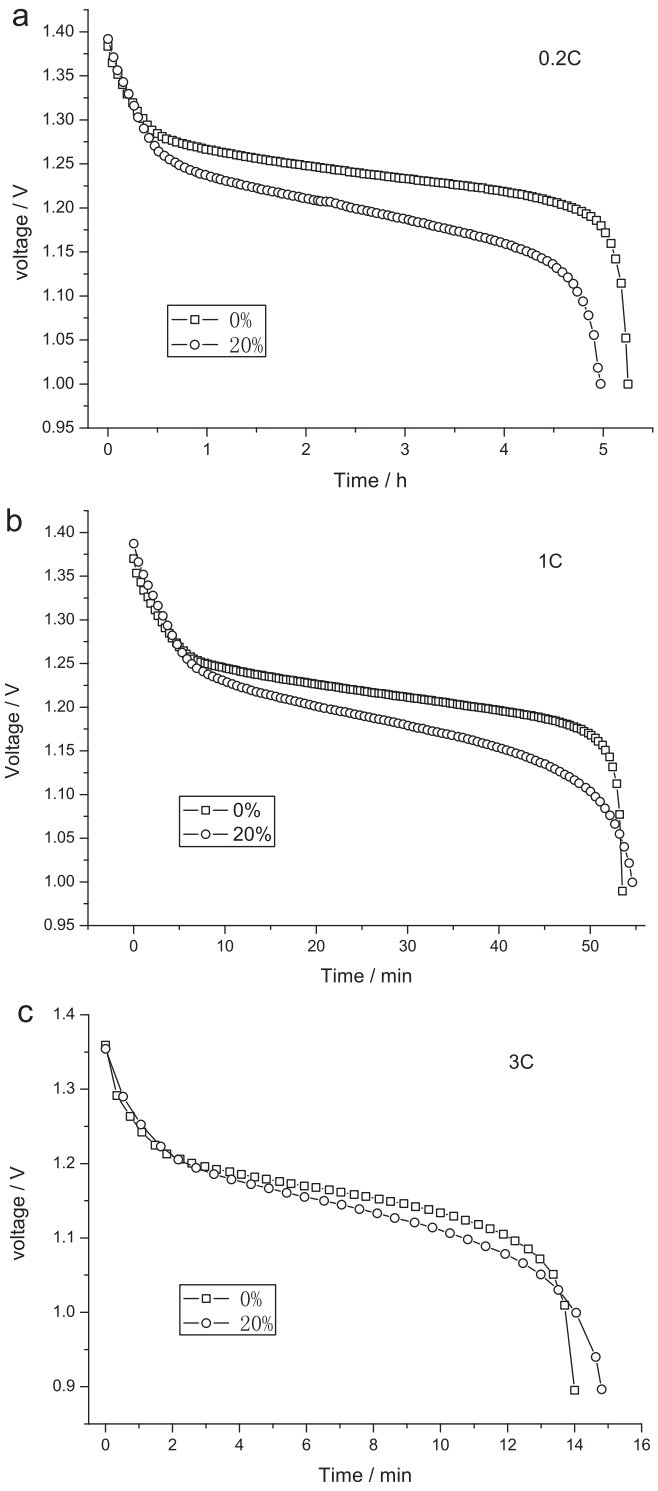

Fig. 10. Typical discharge curves of the simulated Ni-MH batteries at different discharge rates with ball milled nickel hydroxide (a) no-substitution and (b) $Ni_{0.8}Mn_{0.2}(OH)_2$.

According to the following reaction

$$Ni_{0.8}Mn_{0.2}(OH)_2 + OH^- \rightarrow Ni_{0.8}Mn_{0.2}OOH + H_2O + e \quad (2)$$

The theoretical capacity of $Ni_{0.8}Mn_{0.2}(OH)_2$ is 291 mA h/g, which is closed to the theoretical capacity of $Ni(OH)_2$ (289 mA h/g). The 0.2 C capacity of $Ni_{0.8}Mn_{0.2}(OH)_2$ prepared by ball milling in this paper reaches 282 mA h/g and it shows an excellent cycling durability, thus it is suitable for nickel based alkaline secondary batteries.

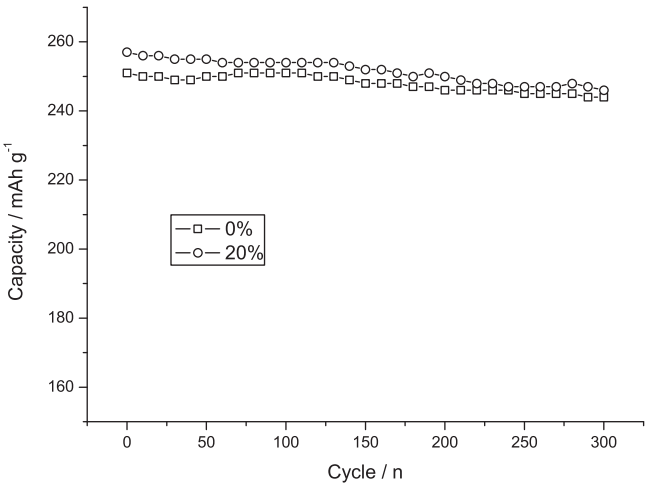

Fig. 11. Capacity of pasted $Ni(OH)_2$ electrodes during 300 cycles at a 1 C rate: (a) no-substitution and (b) $Ni_{0.8}Mn_{0.2}(OH)_2$.

4. Conclusion

A simple ball milling process is used to prepare Mn-substituted nickel hydroxide with low price. XRD analyses show that ball milled Mn-substituted $Ni(OH)_2$ has a structure of β-$Ni(OH)_2$. The substitution amount $x = 0.2$ is chosen for detailed research and the optimal ball milling conditions are obtained as follows: revolution speeds 400 rpm min^{-1}, mass ratio of balls to reaction materials 8:1, milling time for reaction 15 min and drying temperature 100 °C.

Compared to no-substituted nickel hydroxide, $Ni_{0.8}Mn_{0.2}(OH)_2$ shows a decrease both in charge–discharge plateau and capacity at a 0.2 C rate. But with the increase of the discharge rate, the difference in discharge plateau between them is smaller, and the capacity of the latter exceeds the former, since the surface electrochemical activity of nickel hydroxide can be effective improved by Mn substitution as shown in EIS tests.

Acknowledgements

Funding for this work is being provided by Education Department of Henan Province, China through a Research Grant (No. 2009A530006) and Zhengzhou University of Light Industry, China through a Leading Young Teacher Training Grant (201001).

References

[1] A. Taniguchi, N. Fujioka, M. Ikoma, A. Ohta, J. Power Sources 100 (2001) 117–124.
[2] T. Ying, X. Gao, W. Hu, F. Wu, D. Noreus, Int. J. Hydrogen Energy 31 (2006) 525–530.
[3] M. Soria, J. Chacon, J. Hernandez, D. Moreno, A. Ojeda, J. Power Sources 96 (2001) 68–75.
[4] J. Qi, P. Xu, Z. Lv, X. Liu, A. Wen, J. Alloys Compd. 462 (2008) 164–169.
[5] Y. Zhao, J. Wang, H. Chen, T. Pan, J. Zhang, C. Cao, Electrochim. Acta 50 (2004) 91–98.
[6] N. Kosova, E. Devyatkina, V. Kaichev, J. Power Sources 174 (2007) 735–740.
[7] R. Jayashree, P. Kamath, J. Power Sources 107 (2002) 120–124.
[8] Q. Song, C. Chiu, S. Chan, Electrochim. Acta 51 (2006) 6548–6555.
[9] Q. Song, C. Chiu, S. Chan, J. Solid State Electrochem. 12 (2008) 133–141.
[10] H. Chen, J. Wang, T. Pan, H. Xiao, J. Zhang, C. Cao, Int. J. Hydrogen Energy 28 (2003) 119–124.
[11] C. Tessier, P.H. Haumesser, P. Bernard, C. Delmas, J. Electrochem. Soc. 146 (1999) 2059–2067.
[12] T.N. Ramesh, P. Vishnu Kamath, C. Shivakumara, J. Electrochem. Soc. 152 (2005) A806–A810.
[13] W. Hu, X. Gao, D. Norĭeus, T. Burchardt, N. Naksta, J. Power Sources 160 (2006) 704–710.
[14] S. Cheng, W. Leng, J. Zhang, C. Cao, J. Power Sources 101 (2001) 248–252.